Appl. Phys. B 64, 585–591 (1997)

Applied Physics B Lasers and Optics

OH laser-induced fluorescence at high pressures: spectroscopic and two-dimensional measurements exciting the A–X (1,0) transition

B. Atakan[*], **J. Heinze, U.E. Meier**[**]

Deutsche Forschungsanstalt für Luft- und Raumfahrt (DLR), Institut für Physikalische Chemie der Verbrennung, Pfaffenwaldring 38-40, D-70569 Stuttgart, Germany
(Fax: +49-711/6862-578; E-mail: ulrich.meier@dlr.de)

Received: 11 January 1996/Revised version: 25 July 1996

Abstract. Laser-induced fluorescence (LIF) spectra of OH were recorded in the exhaust of a laminar premixed methane/air flame in the pressure range betwen 5 and 36 bar. The OH A–X (1,0) transition near 280 nm was excited. From these spectra, temperatures and effective collisional broadening coefficients were determined by means of a detailed simulation programm. The strong dependence of the pressure broadening coefficient on the rotational quantum number had to be accounted for, in order to avoid systematic errors in the temperature determination. Strategies for temperature measurements at high pressures by two line measurements are presented. In order to demonstrate the applicability of the detection scheme discussed here for high-pressure applications, single-pulse two-dimensional measurements of the OH distribution at 36 bar are presented, as well as an averaged temperature distribution.

PACS: 33.00; 35.00

The majority of technical combustion systems is operated at elevated pressures. Therefore, there is considerable interest in laser-based diagnostic tools in the pressure range between 1 bar and approximately 100 bar. These tools are expected to provide structural information as well as temperatures in turbulent flames; therefore, they have to feature high temporal resolution and, wherever possible, the capability to perform planar measurements.

Compared with atmospheric pressure work, only a few measurements at elevated pressures have been published. Apart from technical problems which arise from making a high pressure environment accessible for laser beams and detection optics, spectroscopic methods that make use of resonant molecular or electronic transitions, like laser-induced fluorescence (LIF) or degenerate four-wave mixing (DFWM), have to deal with several specific difficulties:

– loss of sensitivity due to signal reduction by collisional deactivation (electronic quenching)
– loss of sensitivity due to pressure broadening of absorption lines
– overlapping spectral structures by pressure broadening, resulting in problems with quantitative interpretation (densities, temperature)
– spectral interferences resulting from signals of other species

In recent years, considerable efforts have been made to use LIF detection of the OH radical in flames [1–4] and reacting flows [5] for temperature measurements [1, 4] and flow structure visualization around atmospheric pressure. The hydroxyl radical is attractive for several reasons: It is easily detectable by LIF; it is present in most combustion processes in relatively high abundance; and it is well suited for structural investigations (using planar LIF) and temperature measurements in flames, with the limitation that temperature measurements are restricted to high-temperature regions in flame fronts or hot postflame gases, where OH mole fractions are sufficiently high. Nevertheless, only few experiments have been published about LIF on OH under high-pressure conditions [6–13].

Three UV-LIF detection schemes for OH are frequently used, which differ in the respective vibrational bands used for excitation: the (0,0), the (1,0) and the (3,0) bands of the A–X electronic transition. The (0,0) band has the highest Franck–Condon factor, but the usefulness of this excitation scheme is greatly reduced by absorption and fluorescence trapping problems, at least when flames with large dimensions are investigated. The (3,0) band leads to a predissociating excited state; therefore, the fluorescence quantum yield is very low. This disadvantage can be offset to a large extent using high power tunable excimer lasers. This excitation scheme has been suggested as to be very promising for high pressure conditions because of the reduced sensitivity to quenching, which prevails as long as predissociation is the dominating loss process for population from the laser-excited state, compared to electronic quenching.

There are, however, severe problems associated with this excitation scheme. In a recent joint study performed at the DLR high pressure burner facility, which was also used in the present investigation, it was found by Orth [14] that at pres-

[*]Present address: Universität Bielefeld, Fakultät für Chemie, Universitätsstr. 25, D-33615 Bielefeld, Germany
[**]corresponding author

sures above 15 bar, O_2 fluorescence becomes much stronger than the OH fluorescence, particularly in lean flames, and the OH signal can not be measured unambiguously even by spectral filtering of the detected light. This behaviour is explained by different line broadening coefficients for OH and O_2 in the exhaust of methane/air flames. The only possibility to discriminate between the two spectra is to disperse the fluorescence by a monochromator. Apart from the oxygen interference problem, two issues have to be mentioned which lead to difficulties with the quantitative interpretation of fluorescence signals using the (3,0) band excitation scheme: First, above approximately 10 bar, electronic quenching starts to replace predissociation as the dominating population loss process in the upper state, and secondly, saturation leads to a depopulation of the initial rotational state, which is replenished by rotational relaxation at a rate which depends on temperature, gas composition and pressure.

In the present work, the excitation scheme using the (1,0) transition was employed under high pressure conditions. The aim of this study was to investigate if the problems associated with the other two excitation strategies can be avoided. In addition, effective pressure broadening coefficients in the exhaust of a methane/air flame have been determined, because only very sparse data is available for this transition. The collisional broadening of the OH A–X transition at high temperatures was investigated by Rea et al. [15, 16] for the (0,0) band and by Kessler et al. [17] for the (1,0) band. These groups measured either in shock tubes at pressures of 4.3 bar or in atmospheric pressure flames using narrowband cw laser sources. By changing the stoichiometry and flow rates, broadening coefficients for a few collision partners at several temperatures could be investigated. A significant dependence of the collisional broadening coefficient on the rotational quantum number was found.

In our investigation, we used pulsed laser sources with a bandwidth exceeding by far those of cw lasers; therefore, the pressure range had to be extended significantly in order to obtain linewidths well above both Doppler width and laser linewidth, in order to obtain reliable pressure broadening data. In the present study, no attempt was made to change the flame stoichiometry systematically to evaluate broadening data for different species. The accuracy of such a procedure would have been inadequate. Instead, we restricted our investigations to flames for which reference temperatures measured by CARS and Raman spectroscopy are available [18]. This enabled us to validate the LIF temperature measurements for the investigated flame conditions.

1 Experimental

The laser beam for the OH excitation was generated by a Nd:YAG-pumped frequency-doubled dye laser (Quanta Ray, DCR-2A and Lumonics, YM 1200 and HD 500). The typical pulse energy in the UV around 280 nm was 14 mJ, the typical laser bandwidth was below 0.15 cm^{-1} FWHM. The UV laser beam was expandend to a typical diameter of 7 mm. A laser sheet was formed in all measurements by a cylindrical lens ($f = 300$ mm). The laser beam was attenuated using dielectric filters in order to avoid saturation of the fluorescence signal; the attenuation was chosen according to the varying saturation conditions with changing pressures.

For the pointwise mesurements, the LIF signal was detected by a photomultiplier tube (Valvo XP 2020), time-integrated and – if necessary – averaged by a boxcar integrator (Stanford Research Systems SR250). The integrated and averaged signals were digitized by an A/D-converter (SR245) and recorded by a personal computer. In addition, the laser pulse energy was measured simultaneously before and after passing the flame by vacuum photodiodes (ITT F-4000). The LIF signal was spectrally filtered by three filters (Schott WG 305, Schott UG 11, and an interference filter centered at 309 nm). This combination served as a bandpass filter with peak transmission at 309 nm (FWHM: 16 nm, peak transmission: 5.5%), which transmits mainly red-shifted fluorescence in the (1,1) vibrational band and suppresses stray light very efficiently. In addition, attenuators were used in front of all three detectors to ensure linear operation. The LIF signal was normalized with respect to the laser intensity, which was measured in front of the flame. At pressures above 10 bar, problems arose in the detection of the laser beam after passing the burner because of severe deflection by the flame. However, no significant laser beam absorption within the OH A–X (1,0) band was measured up to 36 bar. Even in the exhaust of a stochiometric CH_4/air flame at 40 bar, the laser beam absorption on the strongest transitions of OH A–X (0,0) band was determined to be less than 10% along the short geometrical dimensions of less than 8 mm.

The planar LIF signal was detected by an intensified CCD camera with 12 bit resolution (LaVision, FlameStar II) through a $f = 105$ mm UV lens (Nikon, UV-Nikkor). A reflex of the laser sheet from a quartz plate was passed through a quartz cell containing a highly diluted dye solution (Coumarin 2 or Rhodamine 6G). The fluorescence from the dye cell, which can be used as a monitor for the spatial intensity distribution in the laser sheet, was recorded simultaneousely by a second CCD camera of the above-mentioned type. From the images of the second camera, a correction function representing the vertical laser intensity distribution was extracted by horizontal integration. This is justified, as long as no significant absorption of the laser beam is observed. In addition, off-resonance images were recorded and averaged. The off-resonance images were subtracted from the raw images, and a normalization was performed by dividing each pixel row of the images by the corresponding relative local laser intensity, as given by the correction function.

A premixed, laminar methane/air flame at various pressures was investigated [19]. The methane/air gas mixture passed through a sintered temperature-stabilized bronze plate with 8 mm diameter. Typical total gas flows were between 1 and 6 slm. A co-flow of cold air around the flame was used for pressure build-up and control. The inner diameter of the burner housing was 60 mm. Four heated quartz windows provided optical access. The equivalence ratio of the flame could be varied between 0.95 and 1.65.

2 Results and discussion

2.1 Excitation spectra

Excitation spectra between 5 and 36 bar were recorded for several spectral regions. There were various aims of this work: To ensure that no other interfering species were ex-

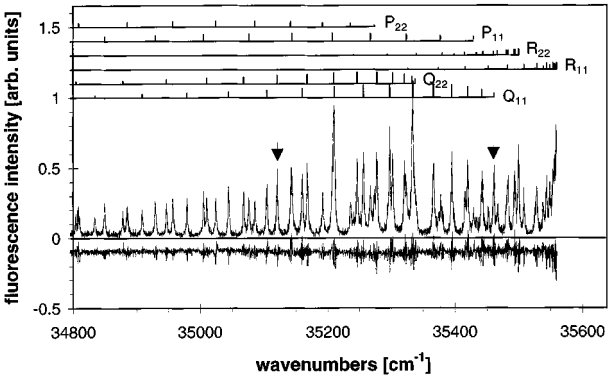

Fig. 1. OH A–X (1,0) LIF excitation spectrum in the exhaust of a premixed laminar methane/air-flame, $\Phi = 0.95$, $p = 36$ bar, one laser shot per point; bottom: residual. Resulting temperature: 2150 K. Arrows indicate lines used for two-line thermometry

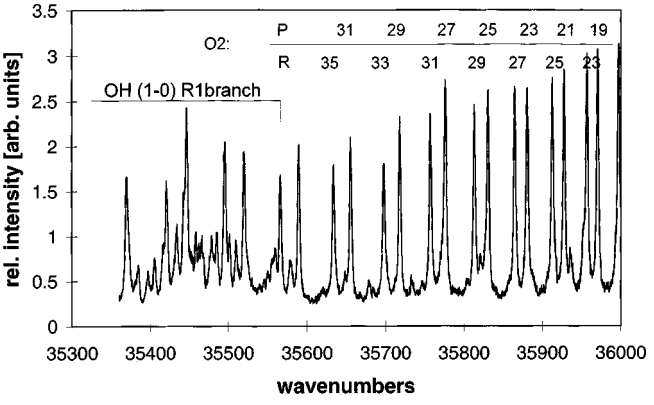

Fig. 2. LIF excitation scan in the region of the OH (1,0) S_{21} branch. CH_4/air flame, $\Phi = 0.73$, $p = 36$ bar. Assignment shows lines in the O_2 B–X (0,9) system

cited in the spectral range between 280 and 287 nm (35700 to 34 800 cm^{-1}), to measure effective collisional broadening coefficients, and to determine flame temperatures. In addition, the single-shot capability of this technique was tested, in view of two-dimensional measurements in turbulent flows. In Fig. 1 a LIF spectrum, which was measured in a slightly lean flame ($\Phi = 0.95$) at 36 bar, is plotted together with the difference between the experimental and a fitted simulated spectrum. The experimental data are not averaged, i.e., only one laser shot was fired per spectral point. From the residual it can easily be seen that no interferences with other molecules occur. A temperature of 2030 K was derived from the fit to this spectrum, in good agreement with Raman and N_2 CARS measurements [18]. The signal-to-noise ratio at the centers of strong lines, which could be deduced from the residual of the fit, was about 6.7. This value is important for the estimation of the statistical error in two-line single shot LIF temperature measurements.

2.1.1 Spectral purity. Neither in slightly rich nor in slightly lean flames any spectral structures which are not due to OH were found in the spectral region shown in Fig. 1, which displays the main P-, Q- and R-branches. The S_{21}-branch in the (1,0) band between 277 and 281 nm (36100 to 35 600 cm^{-1}) is an attractive spectral range for two-line temperature measurements [20], because its rotational lines are relatively widely spaced, which means that temperature measurements are relatively straightforward even at elevated pressures, when lines are strongly pressure-broadened. However, since its lines are more than one order of magnitude weaker than the lines of the P-, Q- and R-branches, this part of the OH spectrum is potentially more susceptible to interferences by other species. Therefore, we inspected this region with regard to interferences particularly in a lean flame, since O_2 was expected to be the main source of perturbations, in analogy to measurements using (3,0) excitation at 248 nm. Figure 2 shows an excitation scan of this part of the spectrum in a lean ($\Phi = 0.73$) CH_4/air flame. The spectral detection window was chosen here deliberately to suppress OH fluorescence by selecting a bandpass filter for the wavelength range 355–400 nm, whereas the OH (1,1) emission peaks around 320 nm. This was achieved with the filter combination UG1 + WG360 + BG40 (Schott). The dominating features in this spectrum are rotational lines of the B–X (0,9) Schumann–Runge system of O_2 [21]. However, if the bandpass filter optimized for OH as described above is used for fluorescence detection, the contribution of O_2 to the signal is of the order of or smaller than the noise on the OH signal baseline. Therefore, the (1,0) band excitation seems to be preferable at elevated pressures in comparison with the (3,0) excitation, where strong O_2 fluorescence interferes with the OH fluorescence.

2.1.2 Saturation. By attenuating the laser intensity, the fluorescence signal was checked for saturation. Alternatively, saturation was also tested by measuring the intensity ratio of different spectral lines originating from the same ground state, but with different rotational line strengths. The intensity ratio of such lines should be equal to the ratio of their line strengths, as long as the transitions are not saturated. At 4.5 bar, selected transitions were partially saturated: For lines with high transition moments, like Q_{11}- and Q_{22}-lines, the saturation parameter [22] $S = I/I_{sat}$ was 0.35 for the strong $Q_{11}(5.5)$ line. The degree of saturation was used as an additional fit parameter and was taken into account in the fitting procedure, as well as saturation broadening. No saturation was observed at higher pressures, because of the p^2-dependence of the saturation intensity: The saturation intensity is proportional to the transversal relaxation, responsible for the linewidth of the transition, and to the longitudinal or population relaxation [23]. Both relaxtion rates scale linear with the pressure.

2.1.3 Line shapes and thermometry. Two spectral ranges of 35 320–35 520 cm^{-1} and 34 820–34 890 cm^{-1} were scanned for each investigated flame with pressures of 5, 9, 18, 27 and 36 bar. The spectral range at longer wavelengths includes many rotational lines with $0.5 \leq J \leq 15.5$. This quantum number range is suitable for temperature measurements with high accuracy, because it includes both states with large rotational energy spacing and lines with good signal-to-noise ratio at the same time. Measured spectra of this part of the spectrum are shown in Figs. 3a and 3b for two pressures. The effect of pressure broadening becomes clearly evident from these spectra. The second spectral range (34 820–34 890 cm^{-1}) features quite isolated lines, so that line shape parameters could be deduced more accurately.

In order to determine flame temperatures and pressure broadening coefficients, a detailed simulation program was used which could fit the temperature, Lorentz bandwidth,

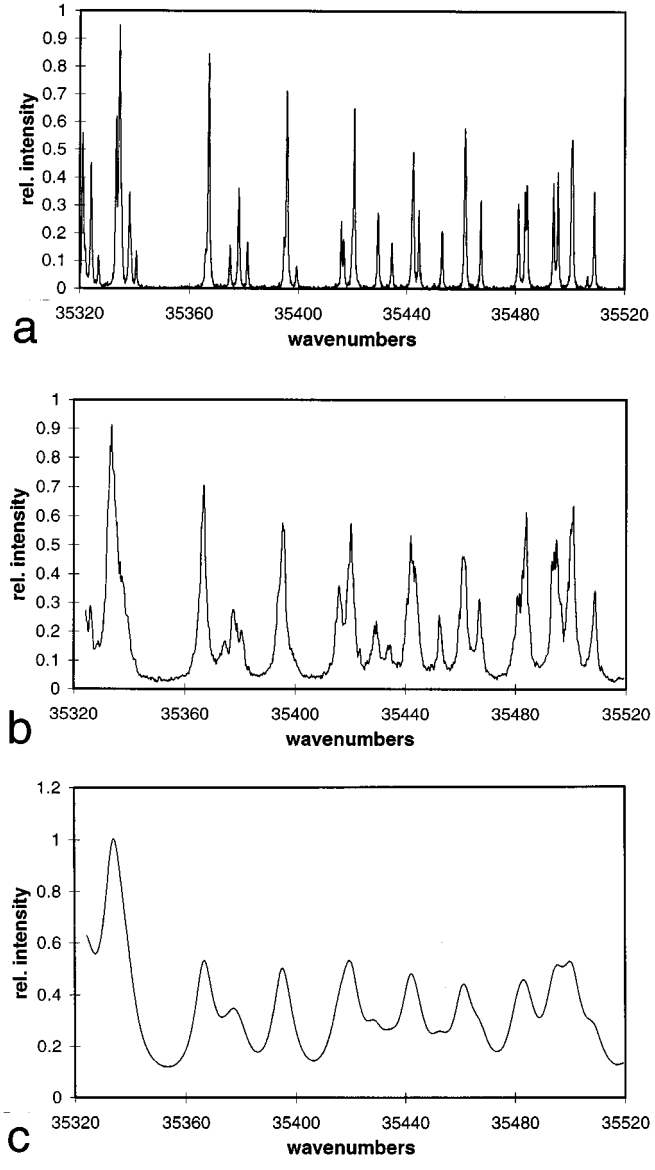

Fig. 3a–c. OH LIF excitation spectra with increasing pressure. **a** at 4.5 bar, $\Phi = 1.05$; **b** at 36 bar, $\Phi = 1.10$. **a** and (**b**): experimental data; **c** simulation for 100 bar

saturation parameter and offset of the spectra by means of a weighted nonlinear least square routine. To simulate a high pressure LIF spectrum for the temperature T, first the population fraction $f_B(T,N'')$ and the transition moment of the rotational line were calculated using the ground state energies of Coxon [24] and the Einstein coefficients of Troller [25]. Then these line strengths were weighted with the relative fluorescence quantum yield of the excited rotational state N': $\eta_{rel}(N',T) = \eta(N',T)/\eta(N'=0,T)$, which was determined by the explicit calculation of the population redistribution in the excited $A(v'=1)$ state due to collision induced rotational and electronic energy transfer, i.e. RET and quenching, respectively [26]. Because of the small variations of the stochiometry in our experiment and the low sensitivity of the relaxation rates with respect to variations in the gas composition, an exhaust gas composition corresponding to a stochiometric flame was assumed for this calculation. Due to the high RET rates in the OH A state, the variation of $\eta_{rel}(N',T)$ with respect to N' is less pronounced than the variation of the relative Einstein coefficient for spontaneous emission, $A_{rel}(N') = A(N')/A(0)$. For example, $\eta_{rel}(N'=11,T=2000\,\mathrm{K}) = 0.96$ and $A_{rel}(N'=11) = 0.86$, respectively. In the next step, each line was convoluted with the homogenous or Lorentzian lineshape, the Doppler width and the laser lineshape to calculate the overlap integral with the laser line shape. The spectral simulation is finished by superimposing all individual lines. The simulated spectra were normalized properly to ensure that the simulated intensities were always proportional to the OH mole fractions, independent of different temperatures and pressures.

In addition, a dependence of the collisional broadening coefficient on the rotational quantum number had to be included, in order to avoid systematic errors in the determination of temperatures. Since the resolution of our spectra did not allow an accurate measurement of this function, we used literature data in the following manner: Rea et al. have measured broadening coefficients k_i for the A–X (0,0) transition of OH in collisions with N_2 [15], H_2O and CO_2 [16] as a function of the rotational quantum number and temperature. We extrapolated their data for the individual collision partners to 2000 K and calculated effective pressure broadening coefficients for the exhaust of a stoichiometric methane/air flame, assuming equilibrium conditions. The effective pressure broadening coefficients $k_{eff}(T)$ were calculated according to the equation:

$$k_{eff}(T) = \sum_i k_i X_i \,, \qquad (1)$$

the mole fraction values (X_i) were taken from isothermal equilibrium calculations for 2000 K. The dependence of k_i on the rotational quantum number N was taken from the data of Rea et al. [15, 16]. This relation could be described by a parabolic function for the relevant N-range ($N < 17$). The coefficients in this parabolic fit are, of course, valid only for the restricted temperature and stoichiometry range of the flame investigated. This relationship is not a fundamental one, but holds for stoichiometric and near stoichiometric methane flames only. The quadratic and linear terms in N were kept fixed in the spectrum fitting procedure, while the constant term was treated as a fit parameter. The pressure broadening coefficients we derived from several fits for different flame conditions are listed in Table 1. The average value was $(0.083 - 0.0026N + 8.0\times10^{-5}N^2)\mathrm{cm}^{-1}/\mathrm{bar}$. This is about 15% higher than the value calculated from the data by Rea et al. [15, 16] for each N. We believe that the main reason for this discrepancy are the different vibrational states excited in our ($v'=1$) and Rea's ($v'=0$) experiments. The uncertainty in our line width data should be caused mainly by variations in temperature and stoichiometry. According to

Table 1. Parameters for the investigated methane/air flames

pressure (bar)	eq. ratio	T(Raman)	T	Lorentz width (1/cm bar)
5	1.00	2185	2071	0.0930
9	1.03	2130	2061	0.0810
18	1.05	2065	2077	0.0760
27	1.11	2040	1960	0.0820
36	1.09	2046	2090	0.0860

the measurements of Rea et al., pressure broadening is very sensitive to changes in temperature and gas composition. The flames which were investigated for the determination of the effective broadening coefficient had stoichiometries between 1.0 and 1.1, as in the former N_2-CARS and Raman measurements which were used as a temperature reference [18]. No data for the collisional broadening of OH by CO could be found in the literature. If this broadening coefficient was very different from the average value of a stoichiometric methane/air flame, this would contribute to the difference with the calculated value. Figure 3c shows the simulation of a spectrum in the same spectral range as in Figs. 3a and 3b, based on the measured broadening coefficients, assuming a pressure of 100 bar.

Using the pressure broadening data as described above, gas phase temperatures were evaluated from the spectra at longer wavelengths. Typically 3 to 10 laser shots per spectral point were averaged. From these spectra, temperatures with an accuracy of better than 5% could be determined. The error is mainly caused by the limited signal-to-noise ratio. Using this procedure, the determined temperatures were in good agreement with earlier Raman and CARS measurements [18], whereas if the rotational dependence was ignored, a systematically higher temperature ($\Delta T = 200$ K) was evaluated. It should be noted, however, that the N-dependence of the pressure broadening coefficients for other important flame species has to be known for an extension of these results to other combustion environments, mainly if two line temperature measurement techniques are to be used.

2.1.4 Two-line thermometry. Because of the importance of 2D single-shot two-line temperature measurement techniques for turbulent combustion systems, a short discussion of a measurement strategy will be given here. The number of isolated rotational lines decreases with increasing pressure, but from a simulation of the spectra for different temperatures at the pressure of interest, temperature sensitive spectral structures of the spectrum can be identified. Because of the decreasing signal level with increasing pressure, only spectral shapes with high fluorescence intensity should be used. In order to find such spectral regions, an entire excitation spectrum at 36 bar was simulated for $T_1 = 1500$ K and $T_2 = 2500$ K, respectively, because all measured temperatures in the investigated flame were expected to fall within this interval. A matrix was calculated from simulations of excitation spectra at different temperatures according to the following formula:

$$R(\lambda_1,\lambda_2,T) = \begin{cases} I_{\lambda_1}/I_{\lambda_2}, & \text{if } I_{\lambda_1} > I_{\max}/4 \wedge I_{\lambda_2} > I_{\max}/4 \\ 0, & \text{else} \end{cases} \tag{2}$$

where λ_i are all (discrete) spectral points within a spectrum, I_{λ_i} are the corresponding fluorescence intensities; $I_{\max}$ is the maximum intensity within an entire spectrum for a given temperature.

Now the maximum of $R(\lambda_1,\lambda_2,T_1)/R(\lambda_1,\lambda_2,T_2)$ was searched. This procedure ensured that a pair of spectral structures was found which exhibits both high temperature sensitivity of the intensity ratio and a high detection efficiency. Using this method, the following spectral structures were chosen: The overlapping $Q_{11}(1.5)$ and $R_{22}(2.5)$ lines at 281.913 nm and the $Q_{22}(9.5)$ line at 284.643 nm (see Fig. 1). These structures were then excited in the two-dimensional temperature measurements.

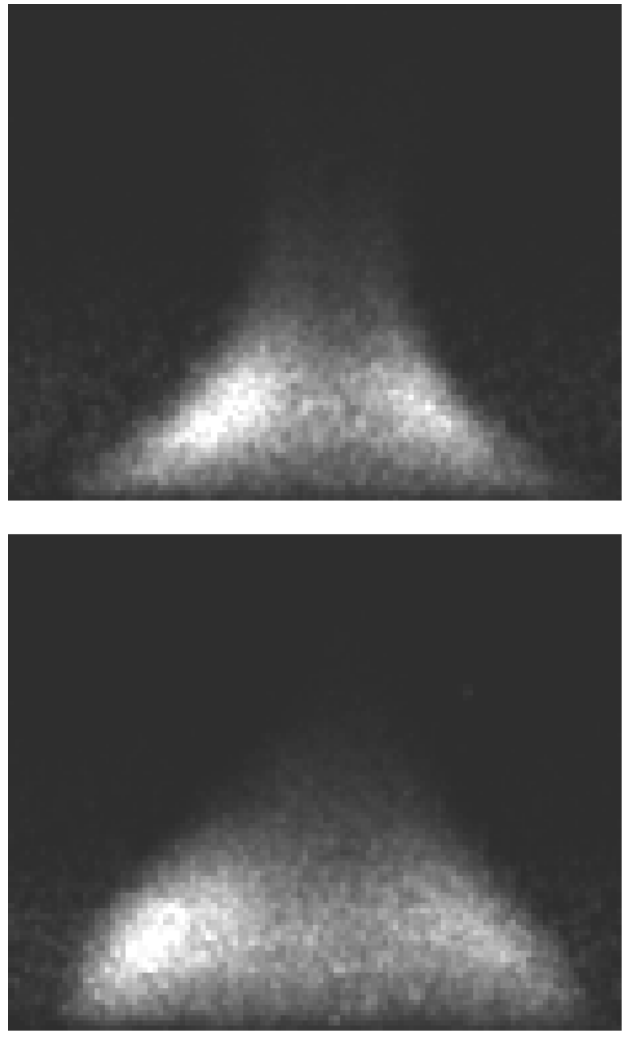

Fig. 4. Two OH density distributions from one series of single-pulse images in a CH_4/air flame at 36 bar, equivalence ratio 1.0

2.2 Two-Dimensional Measurements

Two-dimensional OH distributions were recorded in the entire pressure range between 1 and 36 bar. The following discussion will concentrate on the highest pressure, because demonstration of the feasibility of planar OH LIF at high pressures exciting the A–X (1,0) band was one of the aims of the present work. In addition, this burner is used as a reference burner for high pressure diagnostics. Therefore, the stability and homogeneity of the flame had to be tested, which is easily done with imaging measurements, but very tedious using pointwise techniques. Two single-shot OH distributions for a flame with $\Phi = 1.0$, which were recorded within a few seconds, are shown in Fig. 4. The laser was tuned to 283.220 nm, the main fraction of the signal originates from the $Q_{11}(7.5)$ line which is relatively temperature insensitive in the temperature range of interest. It can easily be seen that the shape

of the OH distributions differs significantly on a shot-to-shot basis. However, the flame is fairly stable temporally and appears to be homogeneous at the position where the Raman and CARS measurements [18] as well as the pointwise LIF measurements were performed. To prove this rather qualitative observation, an averaged image and an image with the local standard deviations from a series of single-shot measurements was calculated. Results obtained from a series of 14 laser pulses are shown in Fig. 5. The labels on the contour lines indicate relative OH densities in the average frame and percent standard deviation in the respective image. The asymmetry in the averaged image may suggest that the laser is absorbed to some degree. However, no evidence for absorption was found even on the much stronger (0,0) band (cf. section 1). In addition, the laser entered the flame from the right side in this experiment, while the highest fluorescence signal is found on the opposite side. The asymmetry is rather a property of the burner itself. From the standard deviation image, it can be seen that the flame exhibits indeed only a small fluctuation ($< 20\%$) at the measurement position for the pointwise techniques, which is located at an axial distance of 1.5 mm above the burner surface and in the center of the flame. Such spatially resolved standard deviations, combined with the averaged image, could be very useful for the investigation of turbulent flames and should reduce the problems in the comparison of theoretical and experimental results in this area of research, because they provide a quantitative information on the degree of local fluctuations.

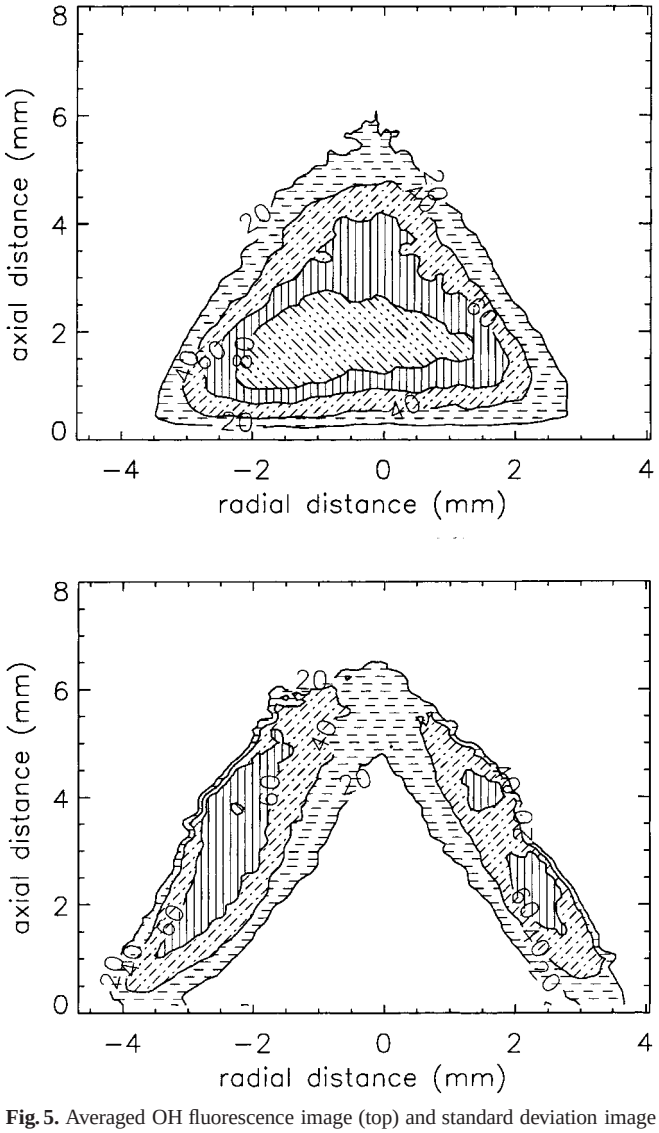

Fig. 5. Averaged OH fluorescence image (top) and standard deviation image (bottom) from a series of 14 single-pulse images. Annotation on contour lines shows std. deviation in percent and relative fluorescence intensity, respectively

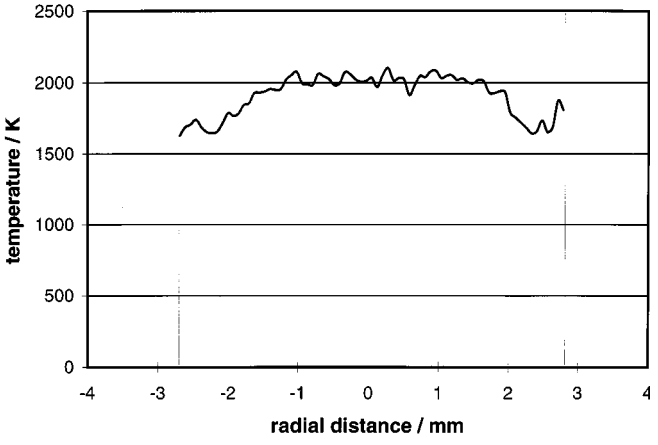

Fig. 6. Radial profile from OH LIF temperature image in a CH_4/air flame at 36 bar, equivalence ratio 1.0, at 1 mm height above burner surface

The signal-to-noise ratio of the OH LIF images is sufficient to perform two-line temperature measurements even on a single-shot basis. Strictly, such measurements require two lasers for the quasi-simultaneous excitation of two lines originating from different rotational states, and two camera systems for the detection of the respective fluorescence. However, since the flame under investigation here was sufficiently stable spatially and temporally at least in its center part, as discussed above, it was legitimate to reduce the experimental effort in this case by exciting the two lines subsequently with just one laser and to average the LIF images on each line for an improved accuracy of the resulting temperature image. Using the procedure described in section 2.1.4., we calculated the average temperature from 14 averaged frames on each excited spectral structure (not line!). A straightforward Boltzmann analysis is not applicable at elevated pressures, mainly because of the increasing line overlap. By simulating the relevant spectral range, all parameters like overlapping lines, pressure broadening, Doppler broadening as well as the convolution of the spectral laser profile with the absorption line were taken into account. This simulation was repeated for a series of temperatures between 800 and 2500 K, which is the intervall in which measureable amounts of OH are expected to be found. For each temperature, the ratio of the intensities of the two spectral structures was calculated. The resulting curve of intensity ratios vs. temperature allows the determination of a temperature from a measured intensity ratio of two spectral structures. A radial profile across the resulting temperature image is shown in Fig. 6. The profile was extracted from the image at an axial position of 1.5 mm above the burner, corresponding to the location of the CARS and Raman reference measurements. The outer portions of the flame, which showed large fluctuations, where clipped in the temperature image, because averaging leads to erroneous temperatures under such circumstances. The resulting temperature

is 2020 ± 75 K; the error quoted is one standard deviation for averaging over a range of 14×14 pixels, corresponding to an area of $1 \times 1\text{mm}^2$ in the flame center area around the measurement position for CARS and Raman experiments. This value is in excellent agreement with CARS and Raman measurements in this flame [18].

3 Conclusions

It was shown in the present work that OH LIF using the A–X(1-0) transition can be used as a sensitive and specific tool for combustion diagnostics at high pressures. If the spectral filtering of the LIF signal is chosen properly, no interferences by O_2 should influence the measurements. No interferences were found in rich flames $\Phi < 1.7$, where the OH mole fraction is quite low; however, it would be useful to expand these measurements to even fuel richer or nearly sooting conditions, for a more rigorous definition of the limits of applicability of this detection scheme.

In addition, it could be shown that temperature measurements using this OH detection scheme are feasible even at high pressures. The rotational quantum number dependence of the pressure broadening coefficient has to be taken into account, in order to obtain correct temperatures. Pressure broadening coefficients for further important colliders, like H_2 and CO, would be needed, in order to transfer this method to other combustion environments. Although isolated rotational lines can still be found at 36 bar, it seems to be a better strategy to analyze spectral structures obtained from simulation for different temperatures, in order to achieve high temperature and detection efficiencies.

Selective two-dimensional LIF OH measurements were perfomed for the first time in a methane/air flame exciting the A–X(1,0) transiton at pressures of up to 36 bar. Two-dimensional OH temperature measurements are possible with an accuracy of approximately 10%. The signal to noise ratio can easily be improved, by using an F/2 instead of the F/4.5 lens system, which was used in the present work. It is intended to use this detection scheme in a 100 bar turbulent H_2/O_2-flame in the near future.

Acknowledgements. The authors gratefully acknowledge financial support by the DARA under Contract No. 50TT9405/3 and by the German Fed. Dept. of Education and Research (BMBF) Contract No. 13N6119/4. The authors appreciate the most productive discussions with Prof. Dr. Th. Just and Dr. W. Stricker, DLR, and Dr. V. Sick, University of Heidelberg.

References

1. K. Kohse-Höinghaus, U.E. Meier: in: *Non-Intrusive Combustion Diagnostics*, K.K. Kuo, T.P. Parr, Eds. Third International Symposium on Special Topics in Chemical Propulsion: Non-Intrusive Combustion Diagnostics; May 10–14, 1993, Scheveningen, The Netherlands, Begell House Inc., New York/Wallingford pp.53–64 (1994)
2. U.E. Meier, R. Kienle, I. Plath, K. Kohse-Höinghaus: Ber. Bunsenges. Phys. Chem. **96**, 1402–1410 (1992)
3. A. Arnold, H. Becker, R. Hemberger, W. Hentschel, W. Ketterle, M. Kollner, W. Meienburg, P. Monkhouse, H. Neckel, M. Schäfer, K.P. Schindler, V. Sick, R. Suntz, J. Wolfrum: Appl. Opt. **29**, 4860–4872 (1990)
4. A. Arnold, B. Lange, T. Bouch'e, T. Heitzmann, G. Schiff W. Ketterle, P. Monkhouse, J. Wolfrum: Ber. Bunsenges. Phys. Chem. **96**, 1388–1393 (1992)
5. M.P. Lee, B.K. McMillin, J.L. Palmer, R.K. Hanson: Journal of Propulsion and Power **8**, 729–735 (1992)
6. P. Andresen, G. Meijer, H. Schlüter, H. Voges, A. Koch, W. Hentschel, W. Oppermann, E. Rothe: Appl. Opt. **29**, 2392–2404 (1990)
7. R. Suntz, H. Becker, P. Monkhouse, J. Wolfrum: Appl. Phys. B **47**, 287–293 (1988)
8. B.E. Battles, R.K. Hanson: J. Quant. Spectrosc. Radiat. Transfer **54**, 521–537 (1995)
9. P. Andresen, H. Schlüter, D. Wolff, H. Voges, A. Koch, W. Hentschel, W. Oppermann, E. Rothe: Appl. Opt **31**, 7684–7689 (1992)
10. A. Koch, H. Voges, P. Andresen, H. Schlüter, D. Wolff, W. Hentschel, W. Oppermann, E. Rothe: Appl. Phys. **56**, 177–184 (1993)
11. K. Kohse-Höinghaus, U.E. Meier, B. Attal-Tretout: Appl. Opt **29**, 1560–1569 (1990)
12. C.D. Carter, N.M. Laurendau: Apll. Phys B **58**, 519–528 (1994)
13. M.G. Allen, K.R. McManus, D.M. Sonnenfroh, P.H. Paul: Appl. Opt. **34**, 6287–6300 (1995)
14. A. Orth: Ph.D. Thesis, University of Heidelberg, Germany (1994)
15. E.C. Rea Jr., A.Y. Chang, R.K. Hanson: J. Quant. Spectrosc. Radiat. Transfer **37**, 117–127 (1987)
16. E.C. Rea Jr., A.Y. Chang, R.K. Hanson: J. Quant. Spectrosc. Radiat. Transfer **41**, 29–42 (1989)
17. W.J. Kessler, M.G. Allen, S.J. Davis: J. Quant. Spectrosc. Radiat. Transfer **49**, 107–117 (1993)
18. W. Stricker, M. Woyde, R. Lückerath, V. Bergmann: Ber. Bunsenges. Phys. Chem. **97**, 1608–1618 (1993)
19. H. Eberius, Th. Just, Th. Kick, G. Häfner, W. Lutz: Proc. Joint Meeting German/Italian Sections of the Combustion Institute; Ravello (Italy) p.3.3 (1989)
20. A. Lawitzki, I. Plath, W. Stricker, J. Bittner, U. Meier, J. Kohse-Höinghaus: Appl. Phys. B, **50**, 513–518 (1990)
21. R.A. Copeland, P.C. Cosby, D.R. Crosley, J.B. Jeffries, T.G. Slanger: J. Chem. Phys. **86**, 2500–2504 (1987)
22. W. Demtröder: *Laser Spectroscopy*, Springer, (Berlin, Heidelberg, New York 1988), p.44
23. K. Shimoda: *Line Broadening and Narrowing Effects in High-Resolution Laser Spectroscopy Topics*, in: Applied Physics Vol. 13 Springer, (Berlin, Heidelberg)
24. J.A. Coxon: Can J. Phys. **58**, 933–949 (1980)
25. M.R. Trolier: Ph.D. Thesis, Cornell University (1988)
26. R. Kienle: Thesis, University of Bielefeld, Germany (1994)